AIAA JOURNAL
Vol. 37, No. 5, May 1999

Technical Notes

TECHNICAL NOTES are short manuscripts describing new developments or important results of a preliminary nature. These Notes cannot exceed 6 manuscript pages and 3 figures; a page of text may be substituted for a figure and vice versa. After informal review by the editors, they may be published within a few months of the date of receipt. Style requirements are the same as for regular contributions (see inside back cover).

Behavior of Airfoil with Control Surface Freeplay for Nonzero Angles of Attack

Denis B. Kholodar* and Earl H. Dowell†
Duke University, Durham, North Carolina 27708-0300

Introduction

In the past few years at Duke University, many studies have been conducted on an aeroelastic wing system with a trailing-edge flap.[1–4] The model here is a three-degree-of-freedom airfoil section with nonlinear structural freeplay in flap rotation. It is based on the state-space model proposed in Ref. 5 and developed in Refs. 1 and 2. The aeroelastic section under study is shown in Fig. 1a. The piecewise linear change in the structural stiffness of the control surface (as shown in Fig. 1b) is the freeplay nonlinearity. Numerical time marching integration determines the system's response (fourth-order Runge–Kutta method) by updating the equations of motion with the use of Hénon's method[6] as the system moves from one linear region into the next. As shown in previous work, results obtained by time integration agree with other theoretical and experimental results.[1–3]

In this Note we use the aforementioned numerical approach to analyze the nonlinear behavior of the system (Figs. 1a and 1b) as the mean or steady angle of attack is being changed. Attention is focused on the transition from small angles of attack to larger angles of attack. Within this transition region, the limit cycle behavior gives way to static equilibrium points over certain velocity ranges as the angle of attack is increased, with a wide variety of nonlinear behavior exhibited in between. The dependence on initial conditions is also considered.

Equations of Motion

Theodorsen[7] derived the general equations of motion for the typical three-degree-of-freedom section; the moments on the entire airfoil are balanced about the elastic axis a (shown in Fig. 1a), the moments on the control surface are balanced about the hinge line c, and finally, the vertical forces are balanced over the entire airfoil. We use Theodorsen's equations cast in the state-space form proposed by Edwards et al.[5]:

$$\dot{\tilde{\boldsymbol{x}}} = \boldsymbol{A}\tilde{\boldsymbol{x}} + \boldsymbol{a} \tag{1}$$

The full state vector $\tilde{\boldsymbol{x}}$ is given by

$$\tilde{\boldsymbol{x}} = \begin{bmatrix} \boldsymbol{x} \\ \dot{\boldsymbol{x}} \\ \boldsymbol{x}_a \end{bmatrix}_{8\times 1}$$

where $\boldsymbol{x} = [\alpha, \beta, h]^T$ has three degrees of freedom: pitch α, flap β, and plunge h. This format includes two augmented states $\boldsymbol{x}_a$ required for Jones's approximation of Wagner's indicial loading function, which yields an approximation to the generalized Theodorsen function. Therefore, $\boldsymbol{A}$ is an 8×8 matrix. It contains the aerodynamic contributions to the inertia, damping, and stiffness matrices and is a function of the freestream velocity $\boldsymbol{U}$. The offset vector $\boldsymbol{a}$ is required because the nominal linear relationship for the control surface restoring moment as a function of flap rotation for the stiffer regions (regions 1 and 3 in Fig. 1b) does not pass through the origin. The coefficient matrix $\boldsymbol{A}$ and the offset vector $\boldsymbol{a}$ will change as the system moves from one region into the next. The general form of the $\boldsymbol{A}$ matrix is

$$\boldsymbol{A} = \begin{bmatrix} \boldsymbol{0} & \boldsymbol{I} & \boldsymbol{0} \\ -\boldsymbol{M}_{\text{tot}}^{-1}\boldsymbol{K}_{\text{tot}} & -\boldsymbol{M}_{\text{tot}}^{-1}\boldsymbol{B}_{\text{tot}} & -\boldsymbol{M}_{\text{tot}}^{-1}\boldsymbol{D} \\ \boldsymbol{E}_1 & \boldsymbol{E}_2 & \boldsymbol{F}_a \end{bmatrix}_{8\times 8}$$

where $\boldsymbol{M}_{\text{tot}}$, $\boldsymbol{B}_{\text{tot}}$, and $\boldsymbol{K}_{\text{tot}}$ are total values of mass, damping, and stiffness matrices composed of structural contributions as well as noncirculatory and circulatory aerodynamic contributions; $\boldsymbol{D}$, $\boldsymbol{E}_1$, $\boldsymbol{E}_2$, and $\boldsymbol{F}_a$ are aerodynamic approximation matrices. More details, as well as the specific form of these matrices, are given in Refs. 1 and 5.

Numerical Results

The physical parameters of the airfoil model come from the model described in Ref. 1. A fourth-order Runge–Kutta method is used for

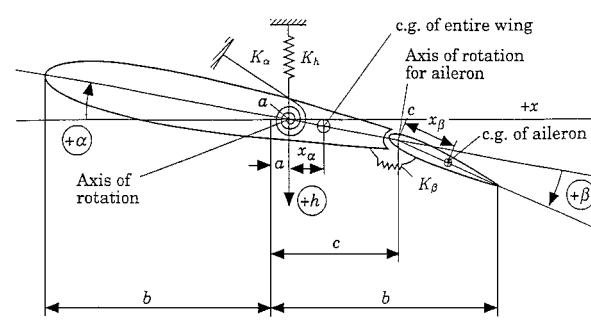

Fig. 1a Sketch of the typical aeroelastic section with control surface.

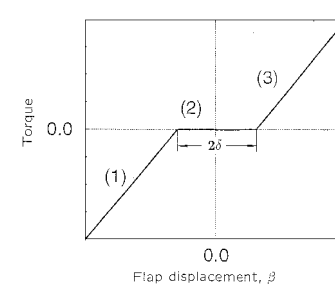

Fig. 1b Restoring moment for the flap degree of freedom β with a symmetric freeplay region about $\beta = 0$.

Received July 28, 1998; revision received Nov. 16, 1998; accepted for publication Jan. 19, 1999.

*Graduate Student, Department of Mechanical Engineering and Materials Science.
†J. A. Jones Professor and Dean, School of Engineering. Fellow AIAA.

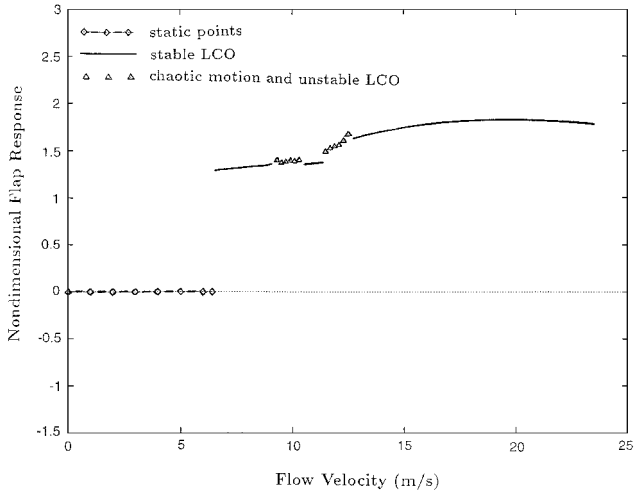

a) $\alpha_0 = 0$

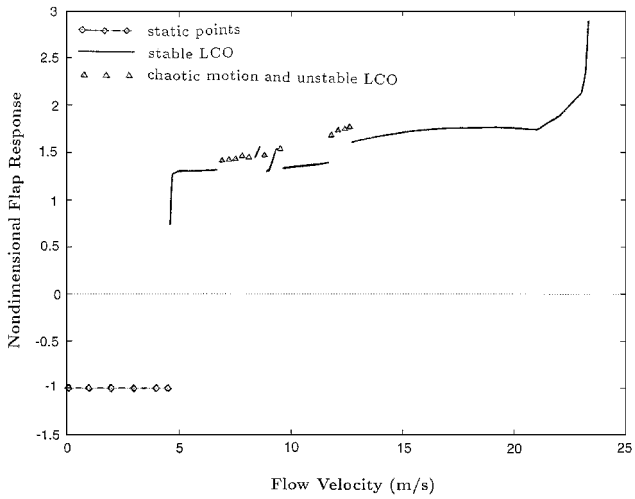

b) $\alpha_0 = 2\delta$

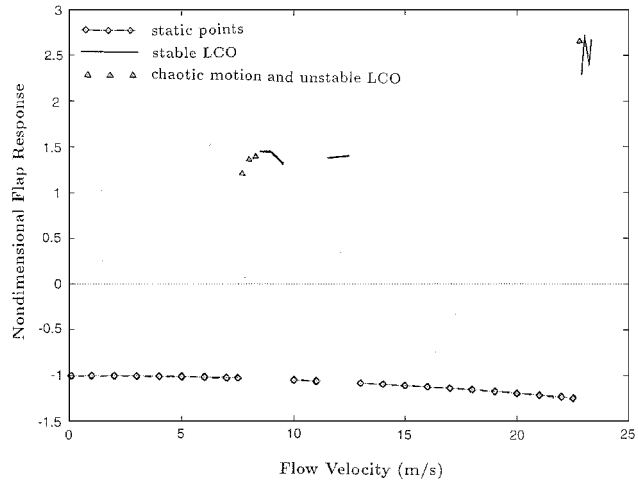

c) $\alpha_0 = 3\delta$

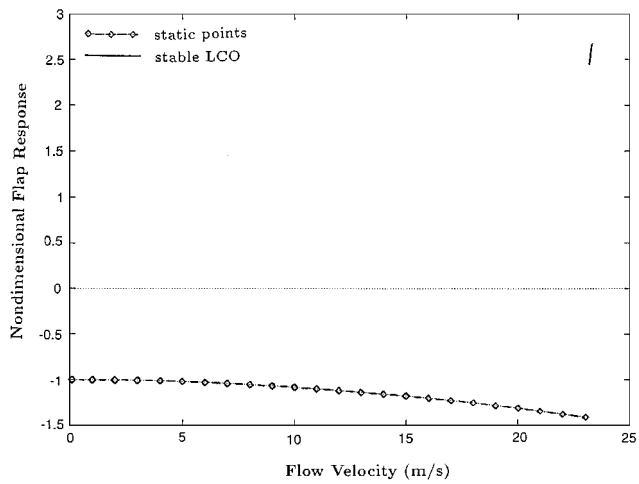

d) $\alpha_0 = 4\delta$

Fig. 2 Nondimensional flap response vs flow velocity for different angles of attack α_0 with initial conditions $x(0) = [0, 2\delta, 0]^T$.

the time integration, where an accurate location of the switching points (on the borders of regions in Fig. 1b) is found with the use of the approach suggested by Hénon.[6] The flap angular motion is used to represent the behavior of the system, and it is scaled in proportion to the freeplay, $\delta = 2.12$ deg, so that the nominal angular gap in Fig. 1b is 4.24 deg; cf. the studies in Refs. 1–4.

As the airflow velocity changes from zero to $U = 23.3$ m/s (just below the flutter velocity of the linear system, $U \cong 23.6$ m/s), three characteristic types of behavior occur (Fig. 2). They are static response, oscillatory behavior with a steady limit cycle, and nonperiodic oscillatory behavior, which can be considered a chaotic motion.

Now consider the results shown in Fig. 2. Here the initial conditions were $\boldsymbol{x}(0) = [0, 2\delta, 0]^T$ and $\dot{\boldsymbol{x}}(0) = [0, 0, 0]^T$. Zero angle of attack was applied for Fig. 2a. Note that α_0 is the angle of attack, whereas $\alpha(0)$ (which is zero in this particular case) is an initial disturbance of the pitch degree of freedom about the α_0. First, note that up to $U = 6.4$ m/s there is a static response, indicated by the line with diamonds. Here the initial disturbance dies out. As the airflow velocity is increased past that value, there is a jump to the limit cycle oscillation behavior indicated by the plain line. For this kind of behavior, the value of the flap response along the vertical axis is a half-amplitude of the limit cycle oscillations (LCO) nondimensionalized by δ. (Half-amplitude is calculated for a limit cycle as the maximum value of β when $\dot{\beta} = 0$, minus the minimum value of β when $\dot{\beta} = 0$ and divided by two.) For a flow velocity of $U = 9.3$ m/s, more complicated nonperiodic behavior occurs. This chaotic behavior is indicated by the triangles. As a measure of the nondimensional response, we calculated a maximum half-amplitude of the flap degree-of-freedom oscillations in a 1-s window averaged over a substantial time interval (divided by δ). At $U = 10.5$–11.4 m/s, there is a small region of LCO, followed by another region of chaotic motion. Finally, as the airflow velocity reaches $U = 12.7$ m/s and up to $U = 23.3$ m/s, another region of LCO takes place. The transitions from one qualitative behavior to another for a zero angle of attack, as well as characteristic details of each region, are discussed in Refs. 1 and 2. Here attention is focused on how the portrayal of the system response changes with respect to changes in the angle of attack.

As the angle of attack increases, the response regions become more fragmented and complicated, as shown in Fig. 2b for $\alpha_0 = 2\delta$. Here the static response ($\beta_{\text{static}}/\delta$, which now is nonzero) is followed by limit cycles for $U = 4.6$–6.8 m/s. Then a region of chaotic motion exists for $U = 6.9$–8.3 m/s. This then gives way ($U = 8.4$–9.5 m/s) to an interval that contains narrow regions of LCO and chaotic motion. Subsequently, at higher velocities, we proceed as before with regions of LCO at $U = 9.6$–11.7 m/s, chaotic motion, and the wide ($U = 12.7$–23.3 m/s) region of LCO.

As the angle of attack is increased further, a qualitatively different situation emerges. For $\alpha_0 = 3\delta$ (as shown in Fig. 2c), we still have a variety of response regions, but the appearance of significant static response regions distinguishes this portrayal from the earlier one.

As the airflow velocity reaches $U = 13$ m/s, the wide region of LCO ceases to exist and gives way to a static response.

As one would probably expect with further increase of the angle of attack, the static response takes over completely, as seen in Fig. 2d for $\alpha_0 = 4\delta$.

Often in nonlinear dynamics it is of interest to study the effects of changes in initial conditions on the system's response. A variety of different initial conditions were tested. The results show that there are some subtle changes in the response of the sytem. For example, an angle of attack of $\alpha_0 = 3\delta$ was considered, and the results were obtained for three sets of initial conditions: $\boldsymbol{x}_1(0) = [0, 2\delta, 0]^T$ (as before), $\boldsymbol{x}_2(0) = [2\delta, 0, 0]^T$, and $\boldsymbol{x}_3(0) = [0, 0, 0.5]^T$. Note that $\dot{\boldsymbol{x}}(0) = [0, 0, 0]^T$ in all three sets. For most of the $\boldsymbol{U}$ interval, there are no substantial differences due to different initial conditions. By this we mean that, for all considered initial conditions, regions of stable LCO, or chaotic motions, or static points begin and end at the same values of the airflow velocity $\boldsymbol{U}$. Also, the numerical values of the response for static points and LCO remain unchanged at least to the second digit after the decimal point, whereas values of the averaged chaotic response may change in the first or second digits after the point. However, in the interval of $\boldsymbol{U} \cong 7$–13 m/s, different initial disturbances lead to the different behavior patterns of the system: The first set of initial conditions produces two small regions of LCO at $\boldsymbol{U} = 8.5$–9.5 and 11.5–12.5 m/s, and the second set results in the dominance of static points, and at the same time, the third set gives rise to an LCO region for $\boldsymbol{U} = 9$–12.8 m/s. For brevity, these results are not shown graphically here, but they are available from the authors.

Conclusions

Using a standard state-space approximation to Theodorsen aerodynamics in a model developed in Refs. 1 and 2, the behavior of a three-degree-of-freedom typical airfoil section has been studied via numerical time integration, with the focus on the effects of the mean or steady angle of attack. A rich variety of nonlinear behavior has been observed; the main tendency displayed by the system as the angle of attack increases was the transition from the predominance of LCOs to a static deflection.

Note, finally, that the magnitude of the flap motion is of the order of the freeplay gap δ. For a typical airfoil, δ is of 1 deg or less. Similarly, the pitch motion is of the order of the freeplay gap δ, and the plunge motion is of the order of the freeplay gap times airfoil chord. Hence, the motions involved are sufficiently small that classical linear aerodynamic theory is still valid, and thus we have used Theodorsen's theory in the present Note. The numerical accuracy of the results shown is well within the dimensions of the symbols plotted in the two figures.

References

[1]Conner, M. D., "Nonlinear Aeroelasticity of an Airfoil Section with Control Surface Freeplay," Ph.D. Dissertation, Dept. of Mechanical Engineering and Material Science, Duke Univ., Durham, NC, 1996.

[2]Conner, M. D., Tang, D. M., Dowell, E. H., and Virgin, L. N., "Nonlinear Behavior of a Typical Airfoil Section with Control Surface Freeplay: One Numerical and Experimental Study," *Journal of Fluids and Structures*, Vol. 11, No. 1, 1997, pp. 89–109.

[3]Tang, D. M., Conner, M. D., and Dowell, E. H., "Reduced-Order Aerodynamic Model and Its Application to a Nonlinear Aeroelastic System," *Journal of Aircraft*, Vol. 35, No. 2, 1998, pp. 332–338.

[4]Tang, D. M., Dowell, E. H., and Virgin, L. N., "Limit Cycle Behavior of an Airfoil with a Control Surface," *Journal of Fluids and Structures*, Vol. 12, No. 7, 1998, pp. 839–858.

[5]Edwards, J. W., Ashley, H., and Breakwell, J. V., "Unsteady Aerodynamic Modeling for Arbitrary Motions," *AIAA Journal*, Vol. 17, No. 4, 1979, pp. 365–374.

[6]Henon, M., "On the Numerical Computation of Poincaré Maps," *Physica D*, Vol. 5D, Nos. 2, 3, 1982, pp. 412–414.

[7]Theodorsen, T., "General Theory of Aerodynamic Instability and Mechanism of Flutter," NACA Rept. 496, 1935.

A. Plotkin
Associate Editor

Further Research for Sensitivity Analyses of Discrete Periodic Systems

Ying Gu,* Lifen Chen,† and Wenliang Wang‡
Fudan University,
200433 Shanghai, People's Republic of China

Introduction

EIGENDERIVATIVES are extremely useful for determining the sensitivities of dynamic responses to system parameter variations. A wide class of physical systems can be approximated by systems of ordinary linear differential equations with periodic coefficients. Unlike the systems with constant coefficients whose sensitivity analysis techniques are well known, the sensitivity analyses of these periodic coefficient equations are somewhat less familiar. In general, the methods developed for the constant systems are not applicable for periodic coefficient systems because the closed form of a Floquet transition matrix is generally unavailable. Usually the finite difference approach is used to calculate the sensitivities. This approach is easy to implement but costly because of heavy computation time. Also, a proper step size is sometimes difficult to determine. Lim and Chopra[1] employed a chain rule differentiation approach to obtain the derivatives of a Floquet transition matrix $\boldsymbol{Q}$ with respect to parameters, which is more efficient than the finite difference approach for calculating the derivatives of the eigenexponents. Later, Lu and Murthy[2] introduced the direct analytical approach, and it made the sensitivity analyses of periodic coefficient systems much more effective. This Note extends the method of Lu and Murthy to the cases in which the period T can be dependent on the system parameters.

Theory of Periodic Coefficient Systems

A general homogeneous, first-order periodic coefficient system is

$$\dot{\boldsymbol{x}}(t) = \boldsymbol{A}(t)\boldsymbol{x}(t) \tag{1}$$

where $\boldsymbol{A}(t)$ is an $n \times n$ periodic matrix, with period T, and $\boldsymbol{x}(t)$ is a column vector of state variables. One set of the solutions of Eq. (1) can be of the form

$$\boldsymbol{x}(t) = \Phi(t)\boldsymbol{x}(0) \tag{2}$$

where $\Phi(t)$ is a standard fundamental solution matrix or state transition matrix. The Floquet theorem[3] states that $\Phi(t)$ can be of the form

$$\Phi(t) = \boldsymbol{P}(t)e^{\boldsymbol{K}t}, \qquad \boldsymbol{P}(0) = \boldsymbol{I} \tag{3}$$

where $\boldsymbol{P}(t)$ is an invertible periodic matrix of order n, with period T, whereas $\boldsymbol{K}$ is a steady $n \times n$ matrix that can be parameter dependent. When $t = T$, we have

$$\boldsymbol{x}(T) = \Phi(T)\boldsymbol{x}(0) \tag{4}$$

From Eq. (3), we obtain

$$\boldsymbol{x}(T) = e^{\boldsymbol{K}T}\boldsymbol{x}(0) \tag{5}$$

Hence,

$$\Phi(T) = e^{\boldsymbol{K}T} \tag{6}$$

Definition: If $\Phi(T)$ and $\boldsymbol{K}$ are the Floquet transition matrix and the steady matrix of a periodic system, then their eigenvalues are said to be multipliers and eigenexponents of the system, respectively.

Received Aug. 20, 1998; revision received Dec. 30, 1998; accepted for publication Dec. 31, 1998.

*Doctoral Candidate, Department of Applied Mechanics. E-mail: ygudx@public6.sta.net.cn.

†Lecturer, Department of Applied Mechanics.

‡Professor, Department of Applied Mechanics.